Relationship between Stiffness of Restorative Material and Stress Distribution for Notch-shaped Non-carious Cervical Lesions

Kwang-Hoon Kim[1], Jeong-Kil Park[2] and Kwon Son[1,#]

1 Department of Mechanical Design Engineering, Pusan National University, Jangjeon-dong, Keumjung-gu, Pusan, South Korea, 609-735
2 School of Conservative Dentistry, Pusan National University, Jangjeon-dong, Keumjung-gu, Pusan, South Korea, 609-735
Corresponding Author / E-mail: kson@pusan.ac.kr, TEL: +82-51-510-2308, FAX: +82-51-512-9835

KEYWORDS: Energy dissipation, Finite element, Non-carious cervical lesion, Restorative material, Stiffness

This study investigated the influence of composite resins with different elastic moduli and occlusal loading conditions on the stress distribution of restored notch-shaped non-carious cervical lesions (NCCL) using 3D finite element analysis. Two different materials, Tetric Flow and Z100, were used as representative flowable hybrid resins for the restoration of NCCL. A static point load of 500 N was applied at the buccal and palatal cusps. The ratios of stress reduction to energy dissipation were better in the compressive state than the tensile state regardless of the restorative material. The total dissipation ratios for Tetric Flow were 1.5% and 4.2% larger than those for Z100 under compression and tension, respectively. Therefore, tensile stress poses more of a risk for tooth fracture, and Tetric Flow is a more appropriate material for restoration.

Manuscript received: January 24, 2008 / Accepted: May 30, 2008

1. Introduction

In clinical dentistry, the loss of hard dental tissue is occasionally observed in the cervical region of a tooth. Erosion, abrasion, and abfraction are the most common contributors to notch-shaped non-carious cervical lesions (NCCLs)[1]. Occlusal loads, which concentrate stress on the cervical area of a tooth, have been thought to cause hard tissue loss at the cementoenamel junction. This is referred to as abfraction by Grippo et al.[2] to distinguish it from lesions caused by erosion and abrasion.

Abfraction lesions are clinically sharp, angular, and wedge-shaped.[3] Abfraction is accelerated by excessive occlusal loads, such as occlusal interference, premature contact, bruxism, and clenching.[4] There are a number of materials that can be used to restore abfraction lesions esthetically. Tooth-colored direct restorative materials are available, including glass ionomer cement, composite resins, and resin-modified glass ionomer. The most appropriate of these is composite resin, despite its disadvantages of time-consuming application, sensitivity to technique, and volumetric shrinkage.[5] Flexible restorative materials are now considered to be better for shear stresses because they are tougher than conventional hybrid composite resins.

Studies of NCCLs have been based on finite element (FE) analysis;[6–8] many of these have only used two-dimensional (2D) analysis and a vertical section of NCCLs. Most studies of the stress distribution of class V cavities have not considered multiple simultaneous factors, such as restorative material, polymerization shrinkage, adhesive layer thickness, and occlusal loading conditions. The purpose of this study was to investigate the influence of composite resins with different elastic moduli and occlusal loading conditions on the stress distribution of a restored notch-shaped NCCL using three-dimensional (3D) FE analysis.

2. Materials and Method

An intact normal extracted human maxillary second premolar was used as a 3D FE model. The extracted tooth was serially scanned with a micro-CT (SkyScan1072: SkyScan, Aartselaar, Belgium) to expose 5.8-μm thick tooth sections perpendicular to the long axis of the tooth and parallel to the occlusal plane. The 3D-DOCTOR image processing software (Able Software Co., Lexington, KY, USA) was used to determine the boundaries of the enamel, dentin, and pulp, and to construct a surface model of the tooth from the sectioned 2D images. ANSYS (Swanson Analysis Systems Inc., Houston, TX, USA) was used to produce meshes and analyze the 3D FE model. Each boundary had an uneven nodal distribution. The corner had more nodes than the center.

The tooth model had three parts: a premolar model with an NCCL, an alveolar bone model, and a restoration model for the notch-shaped lesion. The pulp was not considered because of its much lower density. The model was meshed using 'Smartsize', which is an ANSYS command that can create up to 10 different meshes ranging from 10 (coarse) to 1 (fine); Smart 6 is the default.

The notch-shaped lesion was 4.28 mm high and 5.31 mm wide. The apex of the lesion was placed at the cementoenamel junction (CEJ) and the bone was withdrawn 2 mm under the cavosurface margin of the cervical wall. The lower part of the dentine and the bone model

were joined by a periodontal ligament (PDL). This tooth model was constructed by Smart 6 auto-meshing, and consisted of 177,753 elements with 246,974 nodes. The restored model had 180,095 elements and 249,955 nodes. Figure 1(a) shows a lateral view of the model with an NCCL while Fig. 1 (b) shows its frontal view after restoration. The notch-shaped cavity was filled with a hybrid or flowable resin with a dentin bond thickness of 40 μm.

This study is based on the assumption that all materials remain in their linear elastic ranges. Our interest is in the effect of different stiffness values on the restoration of the lesion. The scope of this study does not cover complicated cases, such as those involving anisotropic properties of enamel and dentine or PDL nonlinearity; this is a potential limitation. The mechanical properties of the tooth and the materials are listed in Tables 1 and 2, respectively.[9–13]

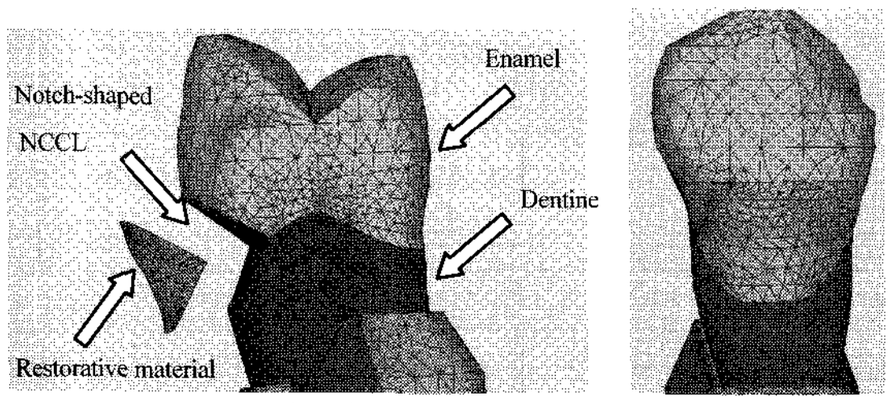

(a) Proximal view (b) Frontal view

Fig. 1 FE model of the notch-shaped NCCL

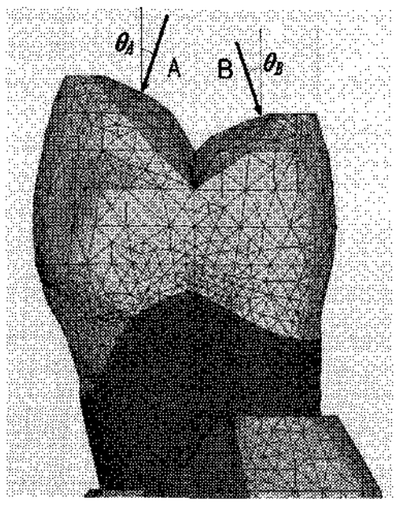

Fig. 2 Loading conditions on the restored tooth with an NCCL (A: Perpendicular load on the upper third of the palatal slope of the buccal cusp. B: perpendicular load on the upper third of the buccal slope of the palatal cusp. Angle θ_A was 27° and θ_B was 19° from the vertical)

Table 1 Mechanical properties of the tooth from (a) Katona et al.,[9] (b) Geramy et al.[10] and Chon et al.[13]

Materials	**Mechanical Properties**	
	Young's modulus (MPa)	Poisson's ratio (υ)
Enamel	84000 (a)	0.33 (a)
Dentin	18000 (a)	0.31 (a)
PDL	0.667 (b)	0.49 (b)
Cancellous bone	13700 (b)	0.38 (b)
Cortical bone	34000 (b)	0.26 (b)

Table 2 Mechanical properties of the materials from (a) Katona et al.,[9] (b) Le S.Y. et al.,[11] and (c) Kleverlaan et al.[12]

Materials	**Mechanical Properties**		
	Young's modulus (MPa)	Poisson's ratio (υ)	Contraction stress (MPa)
Tetric Flow (T)	5300 (a)	0.28 (a)	23.5 (c)
Z100 (Z)	15200 (a)	0.28 (a)	7.6 (c)
Scotchbond MP	1640 (b)	0.28 (b)	-

Two loading conditions were considered for the two restorative materials. Load A was applied perpendicularly on the upper third of the palatal slope of the buccal cusp, and load B on the buccal slope of the palatal cusp (Fig. 2). Both loads were 500 N since some bruxists can produce loads of 500 N or more, and abfraction lesions are known to occur more frequently in bruxists.[3] Tetric Flow (Vivadent Ets., FL-9494-Schaan, Liechtenstein) and Z100 (3M Dental Products, St. Paul, MN, USA) were used as representative flowable hybrid resins. The dentin bonding system used in this study was Scotchbond MP (3M Dental Products, St. Paul, MN, USA). The tooth model had two constraint conditions: the outside surface of the FE model of the alveolar bone was not allowed to move, and the inside surface of the tooth model facing the root was restrained by the PDL.

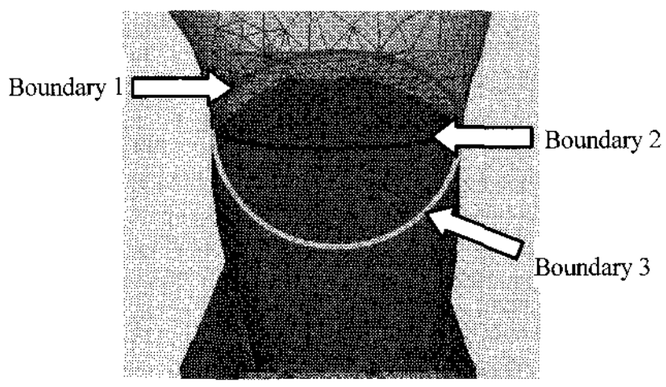

Fig. 3 Boundaries on the cavity wall of the notch-shaped NCCL

Table 3 Mechanical properties of teeth (MPa) from Litonjua et al.[14]

Compressive strength of enamel	277–384
Compressive strength of dentin	249–347
Tensile strength of enamel	10–24
Tensile strength of dentin	32–103

Table 4 Number of elements and total strain energy of different refinement models

Model type	Smart 2	Smart 3	Smart 4	Smart 5	Smart 6
Total strain energy	1460	1463	1459	1456	1457
Elements	236,021	200,970	186,695	181,225	180,095
Energy difference (%)	0	0.21	0.07	0.27	0.21

The von-Mises stresses were analyzed on three boundaries (Fig. 3): the occlusal cavosurface margin (Boundary 1), the lesion apex (Boundary 2), and the cavosurface margin of the cervical wall (Boundary 3). The compressive and tensile strength data of the enamel and dentin are listed in Table 3.[14] The larger value was used as the upper limit and the smaller value as the lower limit for the compressive and tensile strength of each material.

3. Results

Normally, the convergence of FE model results must be verified. In this study, the total energies of the different refinement models were compared to check the convergence. Five models were constructed by changing the size and total number of elements, varying from Smart 2 to Smart 6. The Smart 2 model had the smallest size and the largest number of elements of these five models.

Table 4 shows the number of elements, the total strain energy, and the energy difference of all the models. The energy difference was defined as the percentage compared to the Smart 2 model. The maximum difference was less than 0.3%, which indicates that the Smart 6 model used in this study provides reliable results.

It is clear that the area of the lesion was compressed under Load A and tensed under Load B. Hence, only compressive stresses were considered under Load A and only tensile stresses under Load B. The three boundaries described above were used to obtain the distribution of stress contours, which are shown in Figs. 4 and 5. The stress reduction and dissipation ratios calculated along the boundaries are listed in Tables 5–7.

3.1 Stress distribution

As shown in Fig. 4, the stress is concentrated at the mesial corner under Load A, regardless of the restorative material used. Figure 4(a) shows the stress distribution on the cavity wall before the restoration,

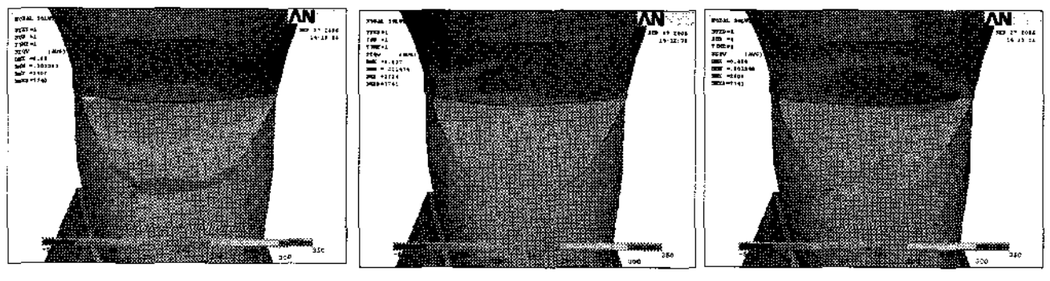

(a) (b) (c)

Fig. 4 Stress distributions on the cavity wall under Load A (a) before restoration, (b) after restoration with Tetric Flow and (c) after restoration with Z100

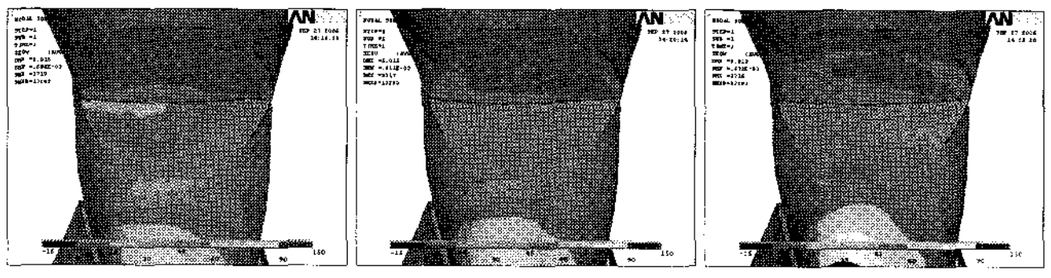

(a) (b) (c)

Fig. 5 Stress distributions on the cavity wall under Load B (a) before restoration, (b) after restoration with Tetric Flow and (c) after restoration with Z100

Table 5 Maximum stresses and reduction ratios

Loading Condition	Cavity	Tetric Flow		Z100	
	Stress (MPa)	Stress (MPa)	Reduction ratio	Stress (MPa)	Reduction ratio
Load A	507	139	72%	128	75%
Load B	179	53	70%	53	70%

Table 6 Number of critical nodes. Load A causes compressive stresses in the lesion area while Load B causes tensile stresses

Classification	Load A (Compression)			Load B (Tension)		
	Cavity	Tetric Flow	Z100	Cavity	Tetric Flow	Z100
Boundary 1	2	0	0	7	5	7
Boundary 2	1	0	0	1	0	0
Boundary 3	1	0	0	1	0	0
Total	**4**	**0**	**0**	**9**	**5**	**7**

Table 7 Summation of squares of stresses and the corresponding energy dissipation ratios (%) on three boundaries

Classification	Load A (Compression)			Load B (Tension)		
	Cavity	Tetric Flow	Z100	Cavity	Tetric Flow	Z100
Boundary 1	748.2	63.2 91.6 (%)	68.7 90.8 (%)	82.4	9.2 88.9 (%)	13.6 83.4 (%)
Boundary 2	697.2	54.4 92.2 (%)	48.0 93.1 (%)	85.6	7.5 91.2 (%)	8.1 90.6 (%)
Boundary 3	378.2	40.8 89.2 (%)	68.3 81.9 (%)	54.0	7.3 86.5 (%)	11.8 78.2 (%)
Total	**1823.6**	**158.4** **91.3 (%)**	**185.0** **89.9 (%)**	**222.0**	**24.0** **89.2 (%)**	**33.5** **84.9 (%)**

and Figs. 4(b) and (c) show it after the restoration with Tetric Flow and Z100, respectively. Before the restoration, dangerous stresses (those greater than 249 MPa in Table 4) were distributed over the lesion apex with a maximum of 507 MPa (Table 5). After the restoration, however, no dangerous stress concentrations were found in the overall lesion area. The maximum stress was 139 MPa for Tetric Flow and 128 MPa for Z100. The stresses were therefore free from danger under Load A, irrespective of the restorative material used.

Similar stress concentration patterns occurred under Load B, as shown Fig. 5. The dangerous stresses that existed at the lesion apex before the restoration (Fig. 5(a)) were reduced to safe levels after the restoration, except at the mesial corner.

3.2 High stress at the mesial corner

This study focused on the stress limits of the dentin and enamel, which are quite different under the loading conditions (Table 4). Table 5 shows the maximum stresses in the boundary area of the lesion and the stress reduction ratios for the two materials before and after the restoration. The reduction is the amount that the maximum stress decreased after the restoration. Under Load A, the reduction ratios were 72% and 75% for Tetric Flow and Z100, respectively; under Load B, they were both 70%. The maximum stress under compression was three times larger than that under tension. However, since the stress limit of compression was much higher than that of tension, the stress distribution under Load A was more stable than under Load B.

To investigate tooth safety, the number of nodes was counted in the boundaries that were over the stress limits (Table 6). Since the three boundaries overlapped at both ends, this overlap was taken into account when calculating the total number of critical nodes. The total number of critical nodes under tension was much larger than that under compression. Table 6 indicates that after the restoration, many nodes still had dangerous levels of stress under Load B while no critical nodes were found under Load A. There were 5 critical nodes for Tetric Flow and 7 for Z100 based on the lower limit under Load B.

3.3 Energy dissipation in the boundaries

To obtain energy dissipation ratios for restorative materials, the boundary energy was defined as the sum of the squares of stresses along that boundary; energy is normally proportional to the square of the stress. The energy dissipation ratio was also defined as the ratio of boundary energy after restoration to that before restoration as follows:

$$\text{Energy Dissipation Ratio (\%)} = \frac{\sum \sigma_{cavity}^2 - \sum \sigma_{restorative}^2}{\sum \sigma_{cavity}^2} \times 100$$

where σ_{cavity} and $\sigma_{restorative}$ are the stresses on the boundaries before and after the restoration, respectively. The square of the stresses represents the total strain energies because the strain energy in the elastic condition is proportional to the product of stress and strain or the square of the stresses. The boundary energies and the corresponding dissipation ratios are listed in Table 7.

The dissipation ratio had the highest value at Boundary 2 (the lesion apex); restoring the lesion is the only effective way to reduce its growth. The total ratio of energy dissipation under Load A was 2.1% larger than that under Load B for Tetric Flow, and 5.0% larger for Z100. Therefore, we know that the energy dissipation was more efficient under compression than under tension. The total dissipation ratios for Tetric Flow were 1.5% and 4.2% larger than those for Z100 under compression and tension, respectively.

4. Discussion

The apex of a notch-shaped lesion is geometrically discontinuous. In general, because of this discontinuity, compressive or tensile stresses are concentrated in this region. Stress concentrations may result in fatigue in the tooth structure and accelerate the progression of abfraction[15]. Therefore, it has been suggested that the severity of the geometric NCCL discontinuity plays a significant role in the development of internal stress in the tooth.

For a tooth with an NCCL, higher stresses are distributed at the apex of the unrestored cervical lesion than at in any other area, regardless of the shape of the lesion[16]. The results of this study lead to similar conclusions concerning stress distribution and intensity at the lesion apex. The higher concentrated stresses cause the cervical area of the tooth to fracture and the lesion to accelerate. The region in

which the higher stresses are concentrated was reduced after restoration because restoration dissipates the intensive stresses.

Many studies have used 2D analysis; however, this study analyzed the stress distribution and concentration on the notch-shaped lesion of NCCL in 3D. The distribution of stress was lower in the tooth restored with the stiffer material because it led to a smaller deformation. However, more flexible material resulted in larger energy dissipation.

The maximum stress of the restored tooth was remarkably less than that of the unrestored tooth. Table 5 shows that the maximum stress in Tetric Flow was larger than in Z100, and that the reduction ratio of compressive stress was slightly larger than that of tensile stress. After restoration, the maximum tensile stresses may result in tooth fracture while the maximum compressive stresses remain far below the danger level. Both Z100 and Tetric Flow have nearly identical reduction ratios for maximum stress. Therefore, it is necessary to restore the NCCL to prevent the abfraction from accelerating.

According to the number of critical nodes (Table 6), tensile stress is obviously a greater risk for fracturing a tooth regardless of whether restoration had been performed. Before restoration, the number of critical nodes was twice as high under tension than under compression. After restoration, the probability of failure was higher for the tooth restored with Z100 than with Tetric Flow. The number of critical nodes for Z100 was higher than that for Tetric Flow.

Enamel has a hardness about five times greater than dentine (Table 1). It is the hardest substance in the body because it has the highest concentration of minerals at about 90%. It is composed of thin rods, known as enamel prisms, that are held together by a cementing substance. This is the reason that enamel is strong to compression but weak to tension. Hence more critical nodes are under tension than in compression at Boundary 1 (Table 6).

The ratio of the energy dissipation under compression was higher than that under tension. The dissipation ratio for Tetric Flow was higher than that for Z100, and the ratio of energy dissipation was the highest at the lesion apex. It is more efficient to restore with Tetric Flow to reduce the total energy in the whole lesion area. On the other hand, Z100 is more useful for reducing the maximum stress. The maximum stresses over the limit may cause the beginning of tooth failure between the restoration and the cavity wall. However, considering that normal biting force (about 170 N) is one-third the abnormal biting force (about 500 N), there was no critical node at the lesion area and so the maximum stress did not exceed the limit.

It is necessary to restore the lesion to prevent abfraction from accelerating. Tetric Flow is better than Z100 for restoring an NCCL because Z100 yielded higher stresses in a wider region than Tetric Flow. This means that Tetric Flow produces less energy in the lesion area. In addition, Tetric Flow may reduce the incidence of tooth fracture due to fatigue.

5. Conclusions

The maximum stress concentration was observed near the mesial corner of the lesion, independent of the restorative materials used or the load conditions. Compared to the untreated cavity, dangerous stresses were significantly reduced for the entire lesion area after restoration. Tensile stresses were considered to be the dominant factor in jeopardizing the restoration durability and in promoting lesion progression. When using only one composite resin material for restoration, the softer material is more efficient than the harder one.

REFERENCES

1. Levich, L. C., Bader, J. D., Shugars, D. A. and Heymann, H. O., "Non-carious Cervical Lesion," J Dent, Vol. 22, Issue 4, pp. 195-207, 1994.
2. Grippo, J. O., Simring, M. and Schreiner, S., "Attrition, Abrasion, Corrosion and Abfration Revisited - A New Perspective on Tooth Surface Lesions," J Am Dent Assoc, Vol. 135, No. 8, pp. 1109-1118, 2004.
3. Rees, J. S., "A Review of the Biomechanics of Abfraction," Eur J Prosthdont Rest Dent, Vol. 7, No. 4, pp. 139-144, 1993.
4. Grippo, J. O., "Abfractions: A New Classification of Hard Tissue Lesions of Tooth," J Esthet Dent, Vol. 3, No. 1, pp. 14-19, 1991.
5. Aw, T. C., Lepe, X., Johnson, G. H. and Mancl, L., "Characteristics of Non-carious Cervical Lesion," J Am Dent Assoc, Vol. 133, No. 6, pp. 725-733, 2002.
6. Ichim, I., Li, Q., Li, W., Swain, M. V. and Kieser, J., "Modelling of Fracture Behaviour in Biomaterials," Biomaterials, Vol. 28, Issue 7, pp. 1317-1326, 2007.
7. Ichim, I., Li, Q., Loughran, J., Swain, M. V. and Kieser, J., "Restoration of Non-carious Cervical Lesions Part I. Modelling of restorative fracture," Dent Mater, Vol. 23, No. 12, pp. 1553-1561, 2007.
8. Ichim, I., Schmidlin, P. R., Li, Q., Kieser, J. A. and Swain, M. V., "Restoration of Non-carious Cervical Lesions Part II. Restorative Material Selection to Minimise Fracture," Dent Mater, Vol. 23, No. 12, pp. 1562-1569, 2007.
9. Katona, T. R. and Winkler, M. M., "Stress Analysis of a Bulk-filled Class V Light-cured Composite Restoration," J Dent Res, Vol. 73, No. 8, pp. 1470-1477, 1994.
10. Geramy, A. and Sharafoddin, F., "Abfraction: 3D Analysis by Means of the Finite Element Method," Quintessence Int, Vol. 34, No. 7, pp. 526-533, 2003.
11. Le, S. Y., Chiang, H. C., Huang, H. M., Shih, Y. H., Chen, H. C., Dong, D. R. and Lin, C. T., "Thermo-debonding Mechanisms in Dentin Bonding Systems Using Finite Element Analysis," Biomaterials, Vol. 22, No. 2, pp. 113-123, 2001.
12. Kleverlaan, C. J. and Feilzer, A. J., "Polymerization Shrinkage and Contraction Stress of Dental Resin Composite," Dent Mater, Vol. 21, No. 12, pp. 1150-1157, 2005.
13. Chon, C. S., Kim, H. S., Shim, J. S. and Kim, Y. H., "Finite Element Analysis for Elastic Modulus of the Periodontal Ligament in Premolar Regions," Vol. 22, No. 10, pp. 202-209, 2005.
14. Litonjua, L. A., Andreana, S., Patra, A. K. and Cohen, R. E., "An Assessment of Stress Analyses in the Theory of Abfraction," Biomed Mater Eng, Vol. 14, No. 3, pp. 311-321, 2004.
15. Grippo, J. O., "Non-carious Cervical Lesions: The Decision to Ignore or Restore," J Esthet Dent, Vol. 4, pp. 55-64, 1992.
16. Kuroe, T., Itoh, H., Caputo, A. A. and Konuma, M., "Biomechanics of Cervical Tooth Structure Lesions and Their Restoration," Quintessence Int, Vol. 31, No. 4, pp. 267-273, 2000.